Hydrate Phase Equilibria of a Near Critical Fluid: Effect of Inhibition and Separation

Kasper K. Østergaard, Bahman Tohidi, Rod W. Burgass, Ali Danesh, and Adrian C. Todd
Dept. of Petroleum Engineering, Heriot-Watt University, Edinburgh EH14 4AS, U.K.

The hydrate phase boundary of a near critical fluid (NCF) was measured at 275–289 K in the presence of distilled water, synthetic formation water, and synthetic formation water with 10.41 wt. % methanol. The results agreed well with the predictions of an in-house model, based on a cubic equation of state and statistical thermodynamics. To simulate a typical oil/gas production scenario, the NCF was flashed at 298.1 K and 17.189 MPa, and the resulting liquid was subsequently flashed at 298.0 K and 4.089 MPa. Hydrate free zones of the resulting liquid fractions were measured to investigate the physical separation effect on the hydrate phase boundary. The in-house thermodynamic model was used to simulate the separators conditions and to predict the hydrate free zone of the resulting liquid and the vapor fractions. The predictions agreed closely with the experimental data, demonstrating reliability of the thermodynamic model. The results also showed that the hydrate phase boundaries of the vapor and liquid phases, which resulted from physical separation, are similar to that of the NCF.

Introduction

Gas hydrates are crystalline inclusion compounds, composed of water and various gas molecules. The water molecules form different sized cavities, some of which are filled and stabilized by the gas molecules. Gas hydrates can form below as well as above the water freezing point at suitable pressure conditions. Gas hydrates have been reviewed in depth by Sloan (1998).

Gas hydrates are of serious concern in petroleum exploration and production due to potential blockage of well-tubing, flowlines, and processing facilities. Major efforts are, therefore, put into development of thermodynamic models which can accurately predict the hydrate free zone of reservoir fluids. This includes the effect of electrolyte solutions (such as formation water) and organic inhibitors (such as methanol and ethylene glycol) on the hydrate free zone. In order to optimize and validate these models, reliable experimental data on the hydrate phase equilibria are needed.

The effect of reservoir fluid production, such as reservoir pressure depletion and surface separation on the hydrate free zone, was modeled in Østergaard et al. (1998). It was shown that after physical separation, the hydrate free zone of the resulting fluids is only subject to minor changes, as compared with the original fluid. This article provides further experimental evidence for the above phenomenon, as well as an extensive set of data on the inhibition effect of formation water and/or methanol on the hydrate phase boundary of a real reservoir fluid.

A near critical fluid (NCF) was chosen for the phase behavior and hydrate studies in this work. The fluid behaved gas-like (gas condensate) at high temperatures and liquid-like (volatile oil) at low temperatures. Near critical fluids could exist in real reservoir conditions, and they represent huge challenges, not only for theoretical phase behavior modeling, but also for experimental fluid behavior studies.

The hydrate dissociation conditions were measured for the NCF in the presence of distilled water, synthetic formation water, and the synthetic formation water with 10.41 wt. % methanol. Furthermore, by adjusting the operating conditions of the experimental equipment, the NCF separation in two-pressure stages was simulated. The hydrate free zones of the two liquid fractions (that is, the liquid fraction of the high-pressure first stage and the subsequent medium-pressure stage) were measured. All experimental data were successfully compared with the predictions of an in-house thermodynamic hydrate prediction model.

Correspondence concerning this article should be addressed to K. K. Østergaard.

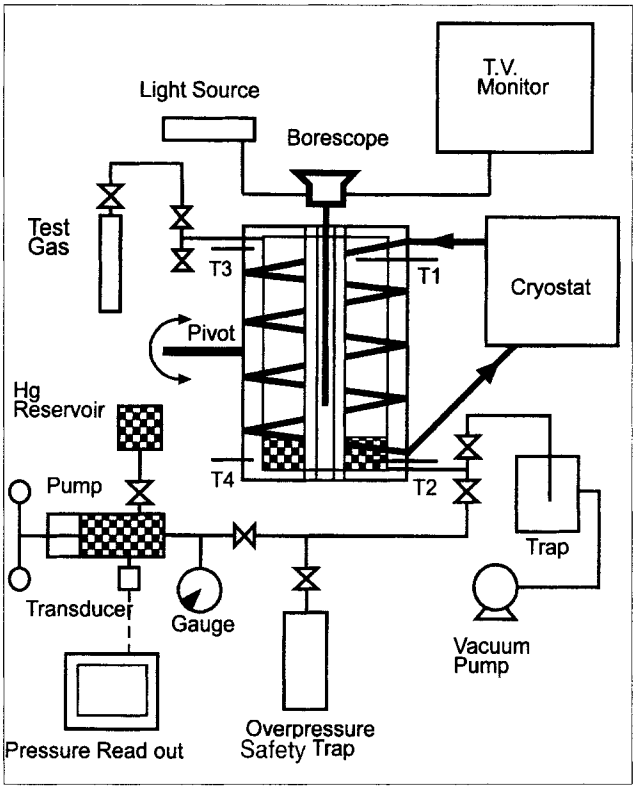

Figure 1. Experimental setup.

Experimental Studies

Test facility

The experiments were performed in a high-pressure hydrate rig, which is shown in Figure 1. The hydrate cell consists of a metal body inside of which an optically clear quartz glass tube is housed. The maximum effective volume of the cell is 540 cc, and the maximum working pressure is 69 MPa. The effective volume is adjusted by injecting or withdrawing mercury. The temperature of the cell is controlled by circulating coolant round a jacket surrounding the cell. The cell is mounted on a pivot, and mixing is obtained by rocking the cell. The pressure and temperature of the system are sampled and recorded at regular intervals. The temperature of the bath is programmed and controlled by a computer. To view the cell contents, a borescope can be passed into the quartz glass tube. A detailed description of the experimental setup is given elsewhere (Danesh et al., 1994; Østergaard et al., 2000). The estimated accuracy of temperature and pressure in the experiments is ± 0.1 K and ± 7 kPa, respectively.

Test fluids

The experiments were performed using a near critical reservoir fluid (NCF). The NCF was prepared in the laboratory by recombining a North Sea stabilized condensate sample and a separator gas sample. The composition of the NCF, determined by gas chromatography, is given in Table 1 together with the molecular weight and the specific gravity (SG) of the single carbon number (SCN) groups. At 373.15 K, the NCF exhibits the behavior of a medium-rich gas condensate with a maximum liquid dropout of 35%, whereas at 298.15 K it behaves like a very volatile oil. The critical point of the NCF is estimated to be around 313 K and 30.8 MPa. Further information on the NCF fluid-phase behavior can be found in Danesh et al. (1997, 1998).

Table 1. Composition of Near Critical Fluid (NCF)*

Component	Mol %	Molec. Wt.	SG @ 288.7 K
N_2	0.36	28.01	
CO_2	0.27	44.01	
C_1	68.73	16.04	
C_2	9.88	30.07	
C_3	4.22	44.10	
i-C_4	0.48	58.12	
n-C_4	1.49	58.12	
i-C_5	0.32	72.15	
n-C_5	0.86	72.15	
C_6's	1.00	84	0.670
C_7's	2.02	89	0.724
C_8's	2.33	103	0.758
C_9's	1.78	114	0.774
C_{10}'s	1.25	132	0.783
C_{11}'s	0.89	148	0.784
C_{12}'s	0.64	165	0.798
C_{13}'s	0.52	177	0.814
C_{14}'s	0.65	187	0.823
C_{15}'s	0.48	204	0.835
C_{16}'s	0.36	218	0.843
C_{17}'s	0.24	234	0.840
C_{18}'s	0.25	250	0.841
C_{19}'s	0.20	262	0.850
$C_{20}+$	0.78	346	0.868

*Average molecular weight: 37.5.
Retrograde dew point: 32.15 MPa at 373.15 K.
Bubble point: 30.13 MPa at 298.15 K.

The synthetic formation water in Table 2 was prepared by weighing the required amounts of salts and distilled water on a balance accurate to ± 0.01 g. The salts (analaR grade) and the methanol (99+% pure) were supplied by Aldrich and the water was double distilled.

Procedure

The test fluids were loaded into the cleaned, dried, and evacuated cell, as detailed below. Distilled water (or formation water, and/or methanol) was pumped into the cell using a HPLC pump from a weighed container giving an accuracy of ± 0.01 g. The NCF was loaded gravimetrically, also with an accuracy of ± 0.01 g. The desired pressure was obtained by adjusting the amount of mercury in the cell.

The mixing of the cell was commenced and the temperature was lowered to form hydrates. The presence of hydrates was visually confirmed by the use of the borescope. The hy-

Table 2. Composition of Synthetic Formation Water

Salt	wt. %
NaCl	12.06
$CaCl_2$	1.04
KCl	0.56
$MgCl_2$	0.12
$SrCl_2$	0.04
$BaCl_2$	0.01

drate formation caused a rapid decline in the pressure of the cell as gas molecules were consumed during the process. The temperature was then increased stepwise, slow enough to allow equilibrium to be achieved at each temperature step (Tohidi et al., 2000). As the temperature increased inside the hydrate region, hydrates would dissociate, causing an increase in the pressure of the cell. This was not the case when the temperature was increased outside the hydrate region. Here, only a small pressure increase was seen due to thermal expansion. Therefore, the point at which the slope of the plot of pressure vs. temperature changed sharply was considered as the hydrate dissociation point. The procedure was repeated at different pressures in order to determine the hydrate phase boundaries over a wide temperature range.

Hydrate phase equilibria were measured for the NCF with distilled water, NCF with formation water, and NCF with formation water and 10.41 wt. % methanol (relative to formation water). All the measured points were in the four-phase L_1-L_2-H-V region, with liquid water (L_1), liquid hydrocarbon (L_2), vapor (V), and hydrate (H) in equilibrium. Furthermore, hydrate phase equilibria were measured on the separator liquid fractions of the NCF in the presence of distilled water, using the following procedure.

In order to simulate a high-pressure (HP) separation, the cell content was equilibriated at 298.1 K and 17.189 MPa, which is outside the hydrate stability region. Next, the vapor phase was removed at constant pressure. The cell pressure and temperature were then adjusted to measure the hydrate phase boundary of the HP separator liquid (in the L_1-L_2-H-V region), using the method described above.

The cell conditions were again adjusted to simulate a second-stage medium pressure (MP) separator operating at 298.0 K and 4.089 MPa. The vapor phase was removed at a constant cell pressure and the hydrate phase boundary of the remaining liquid was measured in the L_1-L_2-H-V and the L_1-L_2-H regions. The composition and the amount of the removed vapor phases in the two stages of separation, as well as the remaining cell contents, were analyzed in order to check the overall material balance. Figure 2 shows the separation conditions and the corresponding fluids. Table 3 presents the compositions of the HP-liquid and the MP-liquid, calculated from the feed composition and the amount and composition of the removed vapor phases. Also in Table 3, the predicted (by the thermodynamic model) amount and composition of the liquid phases are presented. The predictions were made by performing two P-T flash calculations at the separator conditions (as given in Figure 2). A good match between the experimental and predicted fluid compositions is observed.

Results and Discussion

The hydrate dissociation conditions for the NCF with distilled water, formation water, and the formation water plus methanol are given in Tables 4 to 6, respectively. All the data are in the four-phase, L_1-L_2-H-V region. Tables 7 and 8 present the hydrate dissociation conditions for the HP-liquid and the MP-liquid, respectively. These data are also in the four-phase (L_1-L_2-V-H) region, except one high-temperature/high-pressure data point for the MP-liquid, which is in the three-phase (L_1-L_2-H) region. Due to the lack of a free

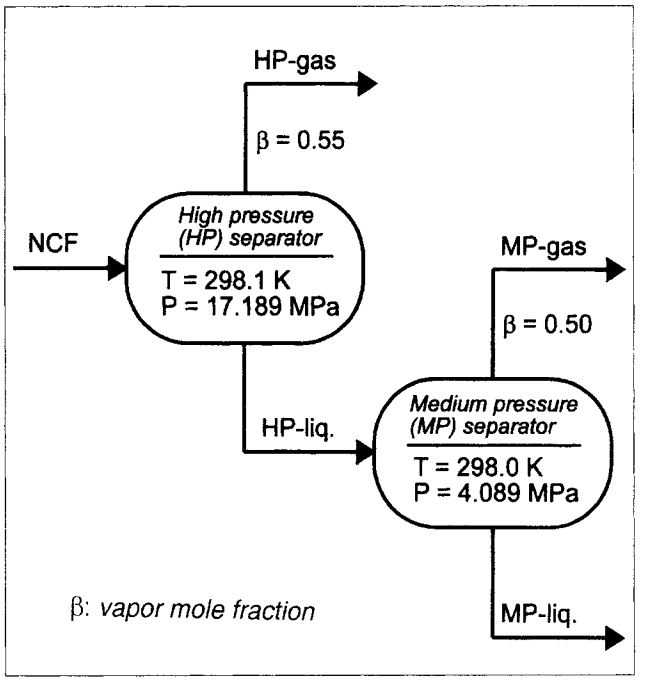

Figure 2. High-pressure (HP) and medium-pressure (MP) separators.

vapor phase, the previously outlined graphical test procedure for determination of the hydrate dissociation point could not be applied. Hence, the high-temperature/high-pressure point

Table 3 Composition of High-Pressure Separator Liquid (HP-Liquid), and Medium-Pressure Separator Liquid (MP-Liquid) in mol %

	HP-Liquid		MP-Liquid	
Component	Exp.	Pred.	Exp.	Pred.
N_2	0.38	0.20	0.37	0.06
CO_2	0.28	0.30	0.27	0.22
C_1	50.04	51.92	16.79	15.15
C_2	10.23	10.92	9.23	9.35
C_3	5.43	5.63	7.70	7.86
i-C_4	0.69	0.70	1.14	1.18
n-C_4	2.26	2.29	3.96	4.05
i-C_5	0.53	0.53	0.99	1.02
n-C_5	1.48	1.45	2.82	2.88
C_6's	1.88	1.75	3.66	3.73
C_7's	4.11	3.69	8.10	8.27
C_8's	4.93	4.44	9.74	10.01
C_9's	3.83	3.46	7.58	7.80
C_{10}'s	2.78	2.48	5.51	5.67
C_{11}'s	1.98	1.79	3.93	4.04
C_{12}'s	1.42	1.30	2.83	2.90
C_{13}'s	1.16	1.06	2.30	2.37
C_{14}'s	1.45	1.33	2.87	2.96
C_{15}'s	1.07	0.99	2.12	2.18
C_{16}'s	0.80	0.74	1.59	1.63
C_{17}'s	0.53	0.50	1.06	1.08
C_{18}'s	0.56	0.52	1.10	1.14
C_{19}'s	0.44	0.41	0.88	0.90
C_{20} +	1.74	1.60	3.46	3.55
β^*	0.55	0.52	0.50	0.51

*Vapor mol fraction.

Table 4. Hydrate Dissociation Conditions for NCF with Distilled Water

T/K (±0.1)	P/MPa (±0.007)
277.2	1.069
280.4	1.627
284.5	2.772
288.4	4.702

Table 5. Hydrate Dissociation Conditions for NCF with the Formation Water

T/K (± 0.1)	P/MPa (±0.007)
276.2	2.103
281.3	4.137
285.2	7.805
287.8	13.914

Table 6. Hydrate Dissociation Conditions for NCF with the Formation Water plus 10.41 wt. % Methanol

T/K (±0.1)	P/MPa (±0.007)
276.3	5.330
280.7	11.349
283.5	24.256

was measured by visual observation, which is in general a less reliable method than graphical determination (Tohidi et al., 1997b).

An in-house thermodynamic model was employed to predict the experimental hydrate dissociation conditions presented in Tables 4 to 8. The statistical thermodynamics model uses the Valderrama modification of the Patel and Teja equation of state for fugacity calculations in all fluid phases (Valderrama, 1990). Salts are modeled by combining the equation of state with a modified Debye-Hückel electrostatic term. The hydrate phase is modeled using the solid solution theory of van der Waals and Platteuw, as implemented by Cole and Goodwin (1990). The Kihara model for spherical

Table 7. Hydrate Dissociation Conditions for HP-Liquid in the Presence of Distilled Water

T/K (±0.1)	P/MPa (±0.007)
278.4	1.193
283.8	2.510
289.3	6.095

Table 8. Hydrate Dissociation Conditions for MP-Liquid in the Presence of Distilled Water

T/K (±0.1)	P/MPa (±0.007)
279.7	1.400
283.3	2.275
287.2	3.944
287.7*	11.721*

*No vapor phase was present and the dissociation condition was measured by visual observation.

Table 9. Kihara Parameters Used in Modeling Hydrate Phase

	α/Å	σ^*/Å[§]	$\epsilon \cdot \kappa^{-1}$/K
C_1	0.2950	3.2512	153.685
C_2	0.4880	3.4315	183.320
C_3	0.7300	3.4900	189.273
i-C_4	0.7980	3.6000	209.577
n-C_4	1.0290	3.4000	195.359
i-C_5	0.9990	4.3000	147.671
CO_2	0.7530	2.9040	171.970
N_2*	0.3350	3.2171	128.390

α: radius of the spherical molecular core; σ: collision diameter; ϵ: depth of energy well; κ: Boltzmann's constant.
*Simple nitrogen hydrates are modeled as sI in the L_1-H-V region (Tohidi, 1995).
§$\sigma^* = \sigma - 2\alpha$.

molecules is applied to calculate the potential function for compounds forming the hydrate phase (the used Kihara parameters are given in Table 9). Detailed descriptions of the numerical modeling can be found elsewhere (Avlonitis et al., 1994; Tohidi et al., 1995). The physical and critical properties of the SCN-fractions in Table 1 were estimated from their measured molecular weights and specific gravities (Riazi and Daubert, 1987) and hydrate structure-II proved to be the stable hydrate structure in all the calculations.

Figure 3 presents the experimental and predicted hydrate phase boundaries for the NCF in the presence of distilled water, formation water, and the formation water with 10.41 wt. % methanol. As seen in the figure, the presence of the formation water and the combined formation water/methanol has a significant inhibition effect on the hydrate free zone of the NCF, that is, about 6.5 K and 12.5 K at 5 MPa, respectively. Furthermore, a very good match between the experimental data and the model predictions is observed, demonstrating the reliability of the thermodynamic model used.

In Figure 4 the experimental hydrate free zone for the NCF and the separator liquid fractions (that is, HP-liquid and MP-liquid) are shown in the presence of distilled water. As

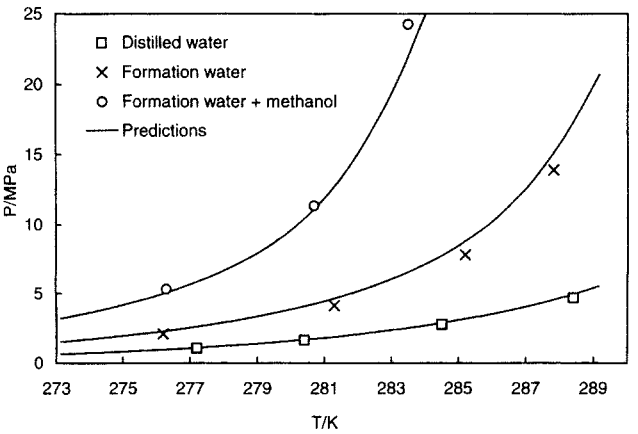

Figure 3. Experimental and predicted hydrate free zones for NCF in the presence of distilled water, synthetic formation water, and synthetic formation water with 10.41 wt. % methanol.

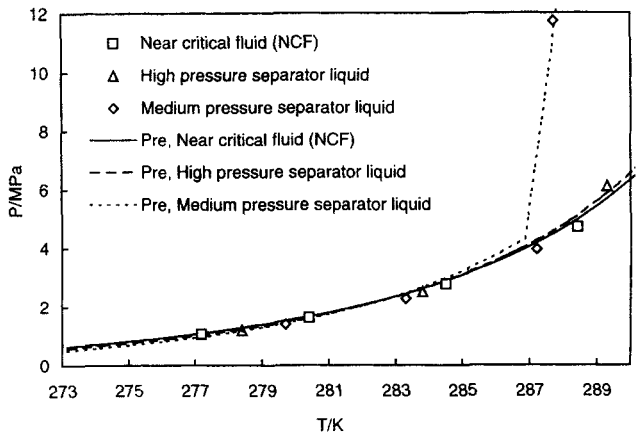

Figure 4. Experimental and predicted hydrate free zones for NCF and its liquid fractions after separation at 298.1 K and 17.189 MPa, and 298.0 K and 4.089 MPa in the presence of distilled water.

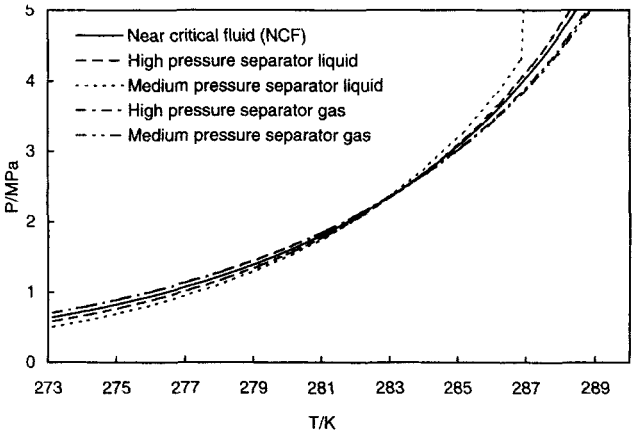

Figure 5. Predicted hydrate free zones for NCF and its fractions after separation at 298.1 K and 17.189 MPa, and 298.0 K and 4.089 MPa in the presence of distilled water.

seen in the figure, the hydrate phase boundaries of the NCF and its subsequent separator liquid fractions are very similar, despite the very different fluid compositions. The hydrate phase boundaries of the liquid fractions follow that of the original NCF in the four-phase (L_1-L_2-V-H) region, up to the bubble point. However, above the bubble point, the hydrate phase boundary of a fluid is a strong function of the temperature. Therefore, the hydrate phase boundary of the separator liquid is different from that of the original fluid in the three-phase (L_1-L_2-H) region. Also in Figure 4, the predictions by the thermodynamic model are shown, demonstrating the reliability and accuracy of the thermodynamic model.

The results in Figure 4 indicate that the hydrate phase boundaries of the NCF and the separator liquids are very similar despite obvious differences in the fluid compositions (Tables 1 and 3). The reason for this peculiar behavior was treated in a previous communication (Østergaard et al., 1998). In brief, however, this is due to the fact that the separation does not have a significant effect on the composition (only on the amounts) of the various phases at the hydrate dissociation temperature and pressure conditions. Furthermore, for fluids with identical phase composition at the hydrate dissociation conditions, the hydrate phase boundaries would also be identical, despite different amounts of the various phases.

In Figure 5 the hydrate free zones (in the L_1-V-H region) of the vapor fractions of the separators are compared with those of the original NCF and the separator liquids. Only predicted phase boundaries are shown, since the hydrate free zones of the separator gases were not determined. However, the comprehensive thermodynamic model has proven reliable in predicting the hydrate free zones of gases (Tohidi et al., 1997a). The hydrate free zones of the separator gases are also very similar to that of the original NCF. Furthermore, when the calculated hydrate dissociation pressure of the separator liquid is lower than that of the NCF, the hydrate dissociation pressure of the corresponding gas is equally higher (and the reverse is true). This observation could be useful when a quick estimate of potential hydrate problems in a production facility is needed.

Conclusion

Experimental and predicted hydrate free zones for a near critical fluid (NCF) have been determined in the temperature range of 275–289 K in the presence of distilled water, a synthetic formation water and the formation water with 10.41 wt. % methanol.

The results show that the formation water and the combination of formation water/methanol have significant inhibition effects on the hydrate phase boundary of the NCF (that is, about 6.5 K and 12.5 K at 5 MPa, respectively).

To investigate the effect of physical separation (used in petroleum industry) on the hydrate phase boundary of reservoir fluids, the NCF was flashed at two stages. The experimental and predicted results showed that the hydrate phase boundaries of the liquid fractions in the four-phase L_1-L_2-H-V region were very similar to that of the original fluid. Also, the predicted hydrate phase boundaries of the vapor fractions (in the L_1-H-V region) were found to be very similar to the original fluid. Therefore, the hydrate phase boundaries of the separator fluids could be estimated from that of the original fluid, saving time and cost in performing experiments and/or modeling.

An in-house thermodynamic model, capable of performing vapor-liquid equilibria as well as hydrate calculations, was employed in predicting the experimental data, with excellent agreement. The result showed that similar predictive models could provide a reliable engineering tool in the economical design and safe operation of pipelines and process facilities prone to hydrate formation.

Acknowledgments

This work has been supported by the Engineering and Physical Sciences Research Council (EPSRC), Amerada Hess Ltd., Deminex UK Oil and Gas Ltd., Health and Safety Executive, Marathon Oil UK Ltd., and Shell U.K. Exploration and Production, which is gratefully acknowledged. The authors wish to thank Alastair Reid for the analysis and characterization of the test fluids, and Jim Pantling for manufacturing and maintaining the equipment.

Literature Cited

Avlonitis, D., A. Danesh, and A. C. Todd, "Prediction of VL and VLL Equilibria of Mixtures Containing Petroleum Reservoir Fluids and Methanol With a Cubic EoS," *Fluid Phase Equilib.*, **94**, 181 (1994).

Cole, W. A., and S. P. Goodwin, "Flash Calculations for Gas Hydrates—a Rigorous Approach," *Chem. Eng. Sci.*, **45**, 569 (1990).

Danesh, A., D. H. Tehrani, A. C. Todd, B. Tohidi, F. Gozalpour, R. Burgass, A. Reid, K. Bell, K. Malcolm, and Z. Al-Siyabi, "Phase Behaviour and Properties of Reservoir Fluids: Reservoir Fluid Sampling and Mixtures," DTI IOR Seminar, London, U.K., (June 17, 1998).

Danesh, A., D. H. Tehrani, A. C. Todd, B. Tohidi, F. Gozalpour, K. Malcolm, A. Reid, K. Bell, K. Elghayed, and R. Burgass, "Phase Behaviour and Properties of Reservoir Fluids: Reliable Tuning of Equation of State with no Binary Interaction Parameters," DTI IOR Seminar, London, U.K., (June 18–19, 1997).

Danesh, A., B. Tohidi, R. W. Burgass, and A. C. Todd, "Hydrate Equilibrium Data of Methyl Cyclo-Pentane With Methane or Nitrogen," *Chem. Eng. Res. & Des.*, **72**, 197 (1994).

Østergaard, K. K., A. Danesh, B. Tohidi, A. C. Todd, and R. W. Burgass, "Effect of Reservoir Fluid Production on Gas Hydrate Phase Boundaries (SPE 50689)," SPE European Petrol. Conf., The Hague, The Netherlands, **2**, 507 (Oct. 20–22, 1998).

Østergaard, K. K., B. Tohidi, A. Danesh, A. C. Todd, and R. W. Burgass, "Gas Hydrate Equilibria of 2,3-Dimethylbutane and Benzene with Methane and Nitrogen," *Chem. Eng. Res. and Des.*, **78**, 731 (2000).

Riazi, M. R., and T. E. Daubert, "Characterization Parameters for Petroleum Fractions," *Ind. & Eng. Chemistry Res.*, **26**, 755 (1987).

Sloan, E. D., *Clathrate Hydrates of Natural Gases*, Marcel Dekker, New York (1998).

Tohidi, B., "Gas Hydrate Equilibria in the Presence of Electrolyte Solutions," PhD Thesis, Heriot-Watt University, Edinburgh (1995).

Tohidi, B., R. W. Burgass, A. Danesh, K. K. Østergaard, and A. C. Todd, "Improving the Accuracy of Gas Hydrate Dissociation Point Measurements," *Annals of N.Y. Academy of Sci.*, **912**, 924 (2000).

Tohidi, B., A. Danesh, and A. Todd, "Predicting Pipeline Hydrate Formation," *Chem. Engr.-London*, **642**, 32 (1997a).

Tohidi, B., A. Danesh, and A. C. Todd, "Modelling Single and Mixed Electrolyte-Solutions and Its Applications to Gas Hydrates," *Chem. Eng. Res. & Des.*, **73**, 464 (1995).

Tohidi, B., A. Danesh, A. C. Todd, and R. W. Burgass, "Hydrate-Free Zone for Synthetic and Real Reservoir Fluids in the Presence of Saline Water," *Chem. Eng. Sci.*, **52**, 3257 (1997b).

Valderrama, J. O., "A Generalized Patel-Teja Equation of State for Polar and Nonpolar Fluids and their Mixtures," *J. of Chem. Eng. of Japan*, **23**, 87 (1990).

Manuscript received June 27, 2000, and revision received Nov. 22, 2000.